NeuroImage: Clinical 27 (2020) 102355

Contents lists available at ScienceDirect

NeuroImage: Clinical

journal homepage: www.elsevier.com/locate/ynicl

Fixel-based analysis reveals fiber-specific alterations during the progression of Parkinson's disease

Yanxuan Li[a], Tao Guo[b], Xiaojun Guan[b], Ting Gao[c], Wenshuang Sheng[a], Cheng Zhou[b], Jingjing Wu[b], Min Xuan[b], Quanquan Gu[b], Minming Zhang[b], Yunjun Yang[a,*], Peiyu Huang[a,b,*]

[a] Department of Radiology, The First Affiliated Hospital of Wenzhou Medical University, 325000 Wenzhou, China
[b] Department of Radiology, The Second Affiliated Hospital, Zhejiang University School of Medicine, 310000 Hangzhou, China
[c] Department of Neurology, The Second Affiliated Hospital, Zhejiang University School of Medicine, 310000 Hangzhou, China

ARTICLE INFO

Keywords:
Fixel-based analysis
Basal ganglia network
Corpus callosum
Cortical spinal tract
Superior cerebellar peduncle

ABSTRACT

Disruption of brain circuits is one of the core mechanisms of Parkinson's disease (PD). Understanding structural connection alterations in PD is important for effective treatment. However, due to methodological limitations, most studies were unable to account for confounding factors such as crossing fibers and were unable to identify damages to specific fiber tracts. In the present study, we aimed to demonstrate tract-specific white matter structural changes in PD patients and their relationship with clinical symptoms. Ninety-eight PD patients, divided into early (ES) and middle stage (MS) groups, and 76 healthy controls (HCs) underwent brain magnetic resonance imaging scans and clinical assessments. Fixel-based analysis was used to investigate fiber tract alterations in PD patients. Compared to HCs, the PD patients showed decreased fiber density (FD) in the corpus callosum (CC), increased FD in the cortical spinal tract (CST), and increased fiber-bundle cross-section (FC, log-transformed: log-FC) in the superior cerebellar peduncle (SCP). Analysis of variance (ANOVA) revealed significant differences in FD in the CST and log-FC in the SCP among the three groups. Post-hoc analysis revealed that the mean FD values of the CST were higher in ES and MS patient groups compared to HCs, and the mean log-FC values of the SCP were higher in ES and MS patient groups compared to HCs. Additionally, the FD values of the CC in PD patients were negatively correlated with the Unified Parkinson's Disease Rating Scale part-III (UPDRS-III) scores (r = -0.257, p = 0.032), Hamilton Depression Rating Scale 17 Items (HAMD-17) scores (r = -0.230, p = 0.033), and Hamilton Anxiety Scale (HAMA) scores (r = -0.248, p = 0.032). Moreover, log-FC values of the SCP (r = 0.274, p = 0.028) and FD values of the CST (r = 0.384, p < 0.001) were positively correlated with the UPDRS-III scores. We concluded that PD patients had both decreased and increased white matter integrity within specific fiber bundles. Additionally, these white matter alterations were different across disease stages, suggesting the occurrence of complex pathological and compensatory changes during the development of PD.

1. Introduction

Parkinson's disease (PD) is the second most common progressive neurodegenerative disorder in people aged above 60. Patients with PD manifest various motor symptoms and non-motor symptoms, such as bradykinesia, rigidity, resting tremor, depression, and cognitive impairment (Braak et al., 2006). The core mechanism of PD is the gradual accumulation of Lewy body in the brain, which damages dopaminergic neurons in the substantia nigra pars compacta. The activation of indirect pathways and inhibition of direct pathways causes imbalance in the basal ganglia network, and leads to motor symptoms (Albin et al., 1989; Alexander and Crutcher, 1990). Additionally, PD pathology also presents in the form of Lewy neuritis, which accumulate in axons and damages white matter connections (Braak et al., 2006). A growing body of evidence suggests that brain circuit changes are the foundation of not only motor symptoms, but also non-motor symptoms such as depression and cognition impairment (Buhusi and Meck, 2005; Huang et al., 2014; Li et al., 2019; Yin and Knowlton, 2006). Therefore, investigating white matter fiber tract alterations may help us better understand the mechanism of PD at the circuit level.

Diffusion tensor imaging (DTI) is traditionally used to investigate white matter fiber integrity changes in PD, and metrics such as fractional anisotropy (FA) and mean diffusivity (MD) were used to reflect the structural integrity of white matter (Beaulieu, 2014, 2002).

* Corresponding authors.
E-mail addresses: yyjunjim@163.com (Y. Yang), hpyzju@foxmail.com (P. Huang).

https://doi.org/10.1016/j.nicl.2020.102355
Received 23 April 2020; Received in revised form 12 June 2020; Accepted 16 July 2020
Available online 20 July 2020

Quantitative comparisons using voxel-based or cluster-averaged metrics were then performed to demonstrate group differences or correlation with disease symptoms (Johansen-Berg and Behrens, 2013). Over the past decade, several DTI studies have reported abnormal microstructures in white matter fibers of patients with PD (Atkinson-Clement et al., 2017; Chan et al., 2014; Gattellaro et al., 2009; Rae et al., 2012). These abnormalities in white matter might be associated with motor symptoms (Vercruysse et al., 2015), impaired executive functions (Rae et al., 2012), color discrimination deficits (Bertrand et al., 2012), cognitive deficits (Hattori et al., 2012; Melzer et al., 2013), olfactory impairment (Ibarretxe-Bilbao et al., 2010), and depression (Li et al., 2010). Although several fiber alterations have been detected using the DTI methods, some of the results may be inaccurate and are difficult to interpret because confounding factors, such as crossing fibers, were not considered. A major limitation of the routine diffusion tensor model is its limited ability to identify diffusivity in complex and crossing fibers, which is present in up to 90% of white matter voxels at the current diffusion tensor image resolution (Jeurissen et al., 2013). When differences are detected in voxels of crossing fiber populations, it is difficult to attribute the alterations to specific fiber pathways (Douaud et al., 2011). Furthermore, if one of the crossing fibers within a voxel has decreased white matter integrity while the other one has increased connectivity, the conventional method may fail to detect both alterations. Therefore, even though the voxel-averaged measures of tensor-derived metrics could reflect abnormalities in certain white matter regions, they are inherently neither fiber-specific nor easily interpretable. Additionally, in neurodegenerative disease conditions such as PD, white matter alterations exist in various forms, such as fiber atrophy and demyelination. The mixture of macro- and micro- structural alterations complicates the crossing fiber issue.

The development of higher-order DTI models make the estimation of multiple fiber orientations within voxels possible (Tournier et al., 2007). A new method called fixel-based analysis (FBA) enables the conduction of fiber-tract-specific statistical analysis (Raffelt et al., 2017), whereby a 'fixel' refers to a specific fiber population within a voxel (Raffelt et al., 2015). Using FBA, we can estimate the orientations of multiple fiber populations within one voxel, and also derive quantitative metrics that can reflect both macroscopic and microscopic fiber changes (Hanaie et al., 2013), including: (i) fiber density (FD), which reflects the density of fibers within a fiber bundle; (ii) fiber-bundle cross-section (FC), which reflects the macro-structural property of fiber bundles; and (iii) fiber density and cross-section (FDC), which reflects a combination of both macroscopic and microscopic degenerative processes. FBA facilitates fiber tract-specific comparisons, in contrast to analyses of voxel-averaged metrics. This method has been used to detect white matter alterations in several diseases, including Alzheimer's disease (Mito et al., 2018), Major Depression Disorder (Lyon et al., 2019), and Multiple Sclerosis (Gajamange et al., 2018), and has been shown to demonstrate good sensitivity and reliability.

In the present study, we aimed to use FBA to investigate white matter fiber alteration in early stage and middle stage PD patients and to explore the association between fiber alterations and clinical symptoms. In several recent *meta*-analysis studies, decreased FA and/or increased MD in the corpus callosum, cingulum, internal capsule, and temporal lobe fiber tracts were found in PD patients (Andica et al., 2019; Atkinson-Clement et al., 2017). Therefore, we expect to find similar alterations. Additionally, although the corticospinal tract (CST) and cerebellar tracts are important motor pathways and were thought to be involved in PD, previous studies reported relatively preserved fiber tract integrity in PD patients (Gattellaro et al., 2009; Lu et al., 2016; Nilsson et al., 2007). With this new methodology, we hope to identify subtle changes in these fiber tracts. Moreover, patients at different disease stages might have different fiber tract alterations, reflecting the pathological features of PD.

2. Materials and methods

2.1. Participants

Seventy-six healthy controls (HCs) and 98 PD patients were recruited from the Department of Neurology, Second Affiliated Hospital of Zhejiang University. PD was diagnosed by a senior neurologist according to the UK PD Brain Bank criteria (Hughes et al., 1992). The exclusion criteria included history of neurological or psychiatric disorders or brain trauma at any point in time in their lives. Scores of the Hamilton Depression Rating Scale 17 Items (HAMD-17), Mini-mental State Examination (MMSE), H&Y stage, the Hamilton Anxiety Scale (HAMA), and Unified Parkinson's Disease Rating Scale part-III (UPDRS-III) were obtained from all subjects by a special scale assessor. The clinical assessments and MR scanning were performed in the OFF condition. Classification of disease stage in PD was typically performed using H&Y staging. Therefore, we divided the patients into two groups (41 PD patients in either the HY1 or HY1.5 stage were collectively called the early stage (ES) group; 57 PD patients in either the HY2 or HY2.5 stage were collectively called the middle stage (MS) group). All the subjects signed written informed consent forms before participating in the study. This study was approved by the Medical Ethics Committee of Second Affiliated Hospital, Zhejiang University.

2.2. Image acquisition and preprocessing

Participants were scanned using a GE Discovery 750 3.0 T MR scanner in the Department of Radiology, Second Affiliated Hospital of Zhejiang University. In order to reduce head motion as much as possible, ear plugs and foam pads were used to prevent noise entry. Otherwise, participants who had claustrophobia, metal implants, or any other situation that makes MRI scan impossible were excluded in this study. Diffusion MR images (dMRI) were acquired with the following parameters: TR/TE = 8,000 ms/minium; acquisition matrix = 128 × 128; field of view = 256 mm × 256 mm; slice thickness = 2 mm, no gap; 67 contiguous axial slices; 30 gradient directions (b = 1000 s/mm^2) with five acquisitions without diffusion weighting (b = 0). Additionally, all patients underwent anatomical T1/T2 imaging, susceptibility imaging, and resting-state functional imaging. The entire acquisition time for each subject was approximately 50 min.

Preprocessing of dMRI included denoising, unringing, motion and distortion correction, bias field correction, and up-sampling dMRI spatial resolution in all three dimensions using cubic b-spline interpolation to a voxel size of 1.3 mm^3 (Raffelt et al., 2012; Tustison et al., 2010; Veraart et al., 2016). Detailed processing steps can be obtained on the MRtrix3 website: https://mrtrix.readthedocs.io/en/latest/. Data was also intensity normalized across all subjects using the median b0 image intensity within a white matter mask. All preprocessing steps were conducted using commands implemented within MRtrix3 (www.mrtrix.org) or using external software packages invoked by MRtrix3 scripts.

Following these preprocessing steps, fiber orientation distributions (FODs) were computed using the Multi-Shell Multi-Tissue Constrained Spherical Deconvolution (MSMT-CSD) method, with group averaged response functions of white matter. Even though the data were single-shell data, we used MSMT-CSD to take advantage of the hard non-negativity constraint, which was demonstrated to produce more robust outcomes (Jeurissen et al., 2013; Tournier et al., 2007). Subsequently, a group-specific population template was created with an iterative registration and averaging approach (Raffelt et al., 2011) using FOD images from 30 subjects (10 ES PD patients, 10 MS PD patients, and 10 HCs). Finally, through an FOD-guided non-linear registration, each subject's FOD image was registered to the template (Raffelt et al., 2012). Additionally, we calculated the values of FD, FC, and FDC for each subject across all white matter fixels. Details of the FBA method and interpretations for generated metrics have been described by

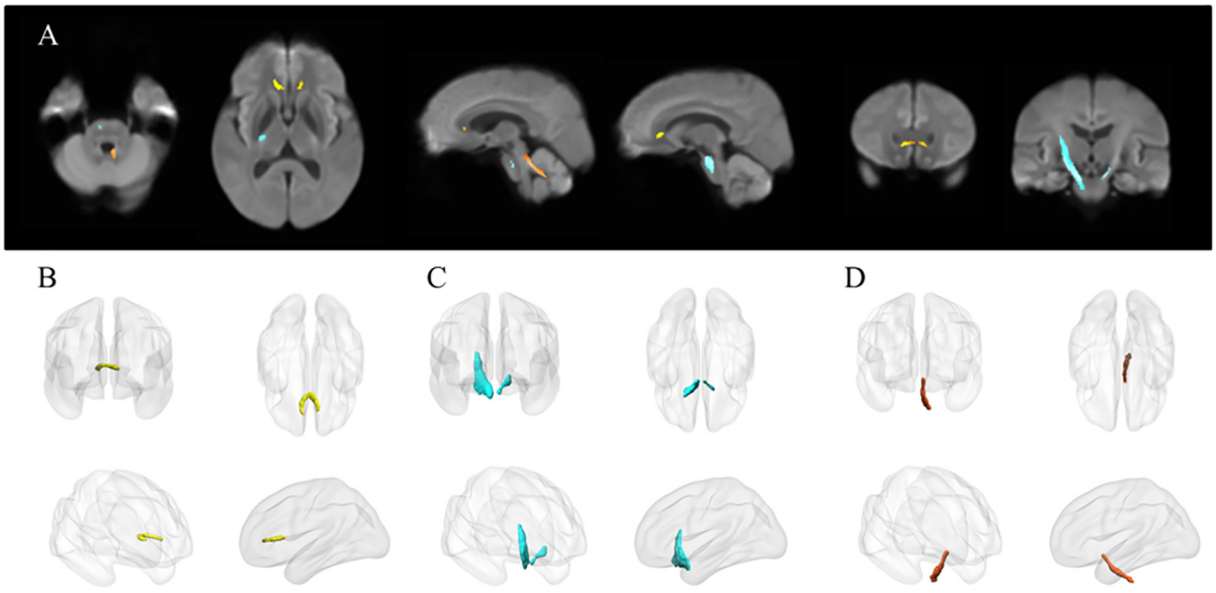

Fig. 1. A. Altered FD or FC regions in the comparison between PD patients and HCs (FWE-corrected, p-value < 0.05). Yellow streamlines represent that HC group have higher FD than PD patients in the genu of CC. Blue streamlines represent that PD patients have higher FD than HC group in the bilateral CST. Orange streamlines represent that PD patients have thicker FC than HC group in left SCP. B-C are the three-dimensional representation of the altered fibers. B shows the genu of CC, C is for bilateral CST and D is for left SCP. (For interpretation of the references to color in this figure legend, the reader is referred to the web version of this article.)

Raffelt et al. (2017). In brief, FD can be generated from transformed FOD images at each voxel based on the Jacobian matrix. FD is sensitive to alterations at the microstructure level. FC can be derived from the warp field calculated from the template to subject space, and is sensitive to fiber atrophy. Moreover, to ensure that the data are centered around zero and normally distributed, we calculated the log-FC instead of the FC for comparison (Raffelt et al., 2017). Similar to the FC, a larger value of log-FC means a larger cross-section. Similar to the template frame of reference, log-FC values > 1 mean a larger cross-section in the subject, and log-FC values < 1 mean a smaller cross-section. FDC is a combination of both FD and FC information and can reflect general fiber alterations. In disease conditions, decreased FC may indicate that the fiber has atrophied, and decreased FD may represent a pathological condition such as gliosis or inflammation (Habas, 2010). Please see Supplementary Fig. 1 for a schematic diagram.

A tractogram was generated using whole-brain probabilistic tractography based on the population template. Twenty million streamlines were first generated and filtered to two million streamlines. Subsequently, the spherical-deconvolution informed filtering of tractograms (SIFT) algorithm was used to reduce reconstruction biases (Smith et al., 2013). Since there was no dedicated fiber tract atlas in MRtrix3, to locate results to specific fibers, we compared the differential fixels with standard brain white matter atlases (Mori et al., 2005; Oishi et al., 2008) and visually identified fiber tracts according to their spatial location and fiber orientations.

2.3. Statistical analysis

Whole-brain comparisons were performed to identify group-differences in FBA metrics. The multiple comparisons correction was performed by combining the connectivity-based fixel enhancement (CFE) method and non-parametric permutation testing, which showed (Raffelt et al., 2015) good control of family-wise errors (FWE). An FWE-corrected threshold of $p < 0.05$ was used to determine significance.

General linear models (GLM) were used to perform group-comparisons, with age, gender, and education included as nuisance covariates. Firstly, t-tests were performed to examine the whole brain fixel differences in FD, log-FC, and FDC between the pooled PD and HCs. Secondly, analysis of variance (ANOVA) tests on FBA metrics were performed among the HCs, ES group, and MS group.

Mean FD and log-FC values were extracted from all participants for further post-hoc analysis based on the results of ANOVA tests. Specifically, a MRtrix3 command was used to threshold the statistical images and construct fixel masks from significant clusters in the ANOVA tests, and the masks were then used to extract the average FD or log-FC value for each subject. Finally, correlation analysis was performed to explore the association between fiber tract alterations and clinical symptoms. The Pearson's method was used to calculate the correlation between mean FD/log-FC values in the significant regions and clinical scales. Additionally, we extracted the mean FD values of the genu of the CC (gCC), which were significantly different between the PD patients and HCs, for further correlation analysis. Bonferroni and FDR correction were used for post-hoc comparison and correlation analyses, respectively.

3. Results

3.1. Clinical and demographic characteristics

As demonstrated in Table 1, PD patients and HCs did not significantly differ in age, gender, and years of education. There were significant differences in HAMA ($p < 0.001$), HAMD-17 ($p < 0.001$), MMSE ($p = 0.004$) and UPDRS-III ($p < 0.001$) scores between HCs and PD patients. There was no significant difference in gender ($p = 0.419$) and years of education ($p = 0.058$), and the HAMD-17 ($p = 0.095$) and HAMA ($p = 0.063$) scores between ES and MS PD patients. The age ($p < 0.001$) and UPDRS-III ($p < 0.001$) score were higher in MS patients than in ES patients. Additionally, the MMSE score ($p = 0.932$) was not different between ES and MS PD patients.

3.2. Whole brain fixel-based analysis

3.2.1. Two sample t-test between pooled PD patients and HCs

Fig. 1 shows the streamline segments after FBA. The FD in the gCC was significantly decreased in the PD patients compared to the HCs. PD patients also showed increased FD in the bilateral CST and increased log-FC in the left superior cerebellar peduncle (SCP) compared to HCs. When macro- and micro- structural fiber alterations were combined

Table 1
Clinical and demographic data of participants.

Index	ES	MS	HC	p value	
				HC vs. PD	ES vs. MS
age	56.08 ± 7.43	61.46 ± 7.75	60.3 ± 6.94	0.346	0.001*
gender	21/20	24/33	47/29	0.422†	0.419†
Years of education	9.51 ± 4.05	7.86 ± 4.32	9.64 ± 2.82	0.057	0.058
HAMD-17	3.76 ± 3.70	5.33 ± 4.35	2.96 ± 3.90	< 0.001*	0.095
HAMA	4.59 ± 4.04	6.18 ± 5.30	2.07 ± 2.70	< 0.001*	0.063
UPDRS-III	13.68 ± 4.89	29.88 ± 12.76	0.54 ± 1.16	< 0.001*	< 0.001*
MMSE	27.17 ± 2.85	27.23 ± 3.55	28.33 ± 1.68	0.004*	0.932

† for chi-square, others were *t*-test.
* $p < 0.05$.

using the FDC metric, an increase in FDC was detected in the bilateral CST of PD patients. Since the area that showed differences in FDC was similar to the area that showed increased FD, we did not include additional figures.

3.2.2. ANOVA tests among HC, ES, and MS groups

Fig. 2 shows that FD and FDC of the right CST, and log-FC of the left SCP were significantly different among the three groups.

3.3. Post-hoc analysis

ANOVA revealed significant differences in the mean FD and log-FC values in fixels (Fig. 3). Bonferroni correction was used for post-hoc analysis. As shown in Table 2, the mean FD value of the CST of ES PD patients (mean = 0.723, SD = 0.057) was higher than that of the HCs (mean = 0.683, SD = 0.066), and the mean FD value of the CST of MS PD patients (mean = 0.759, SD = 0.068) was the highest among the three groups. The differences between the ES group and HCs ($p = 0.004$) and between the MS group and HCs ($p < 0.001$) were significant. The mean log-FC value of the SCP of MS PD patients (mean = -0.016, SD = 0.084) was the highest, followed by that of ES PD patients (mean = -0.025, SD = 0.078), and that of HCs (mean = -0.083, SD = 0.073). The differences between ES patients and HCs ($p < 0.001$) and between MS patients and HCs ($p < 0.001$) were significant.

3.4. Correlation analysis between imaging metrics and clinical scales

As shown in Fig. 4 and supplementary Table 1, mean FD values of the gCC of PD patients were negatively correlated with the UPDRS-III scores ($r = -0.257$, $p = 0.032$), HAMD-17 scores ($r = -0.23$, $p = 0.033$), and HAMA scores ($r = -0.248$, $p = 0.032$). The mean log-FC values of the SCP of PD patients were positively correlated with the UPDRS-III scores ($r = 0.384$, $p < 0.001$). Additionally, the FD values of the CST of PD patients were positively correlated with UPDRS-III scores ($r = 0.274$, $p = 0.028$).

4. Discussion

In the present study, we applied a novel fixel-based analytical method to investigate fiber tract alterations in PD patients. Both increased and decreased white matter integrity were found in specific fiber bundles of PD patients. Additionally, these alterations were associated with motor impairments and were different across disease

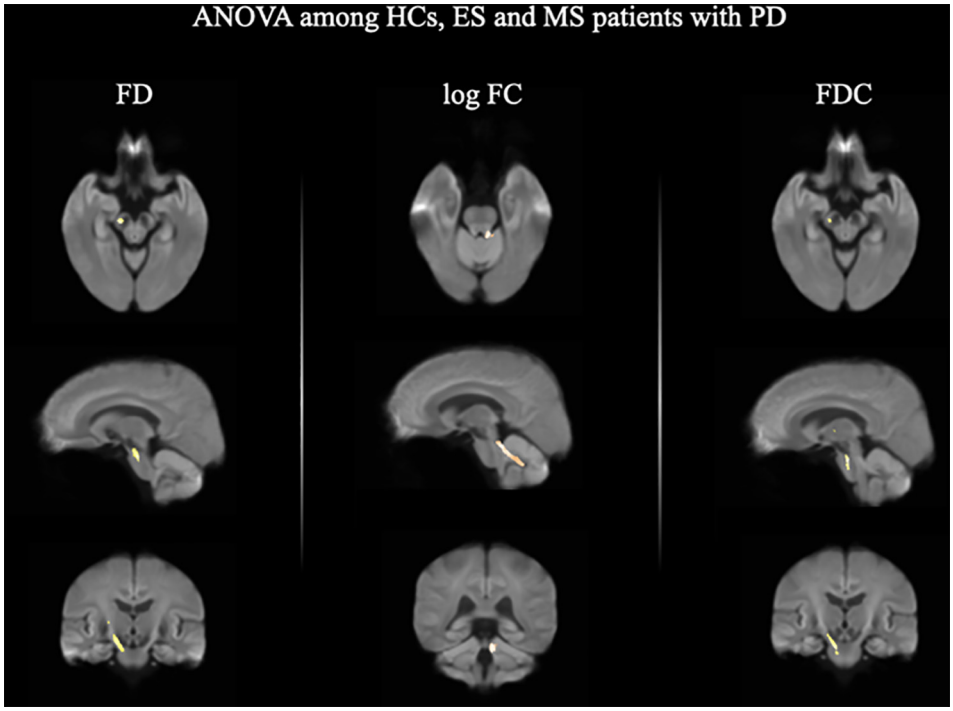

Fig. 2. Fixel abnormalities among ES PD patients, MS PD patients and HCs (FWE-corrected, p-value < 0.05). FD and FDC of right CST and log FC of left SCP were significantly different among the three groups.

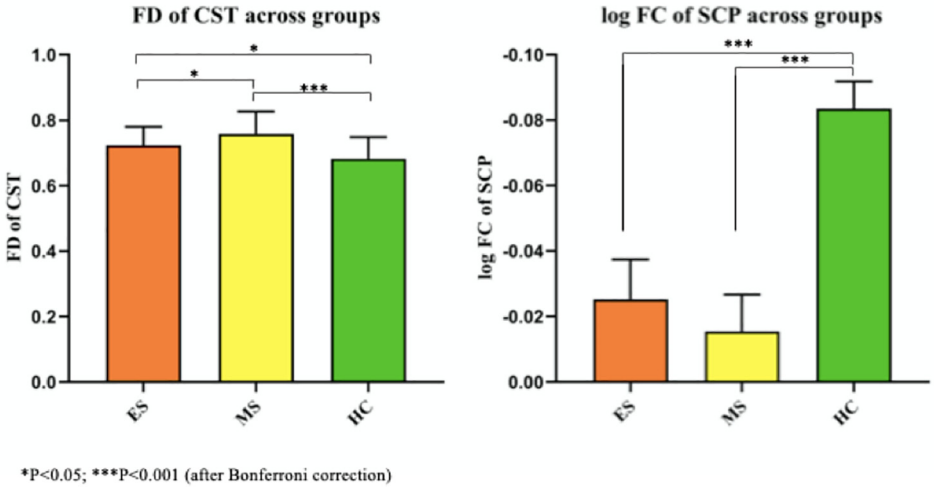

Fig. 3. Results of post-hoc pair-wise comparisons of mean FD values and log FC values extracted from the significant fixels after ANOVA analysis.

stages. These findings could help us better understand brain-circuit changes in PD and potentially help in the diagnosis and treatment of PD.

The implementation of FBA enables the identification of white matter changes within specific fiber bundles. Significant FD reduction was observed in the gCC in all PD patients compared to HCs, reflecting axonal loss at the microstructure level (Raffelt et al., 2017). Although the result had not been found in ANOVA tests, possibly due to the lack of statistical power, it is consistent with several previous studies showing that the white matter integrity of gCC was decreased in PD patients (Gattellaro et al., 2009; Karagulle Kendi et al., 2008). Additionally, we also found a significant negative correlation between the mean FD values of the gCC and motor symptoms, indicating a possible contribution of frontal circuit dysfunction to motor symptoms. The gCC connects the bilateral prefrontal lobes (Innocenti et al., 2002; Yamauchi et al., 1997), which are important for cognitive and motor executive functions (Funahashi and Andreau, 2013; Owen, 1997; Tanji et al., 2007; Zhao et al., 2016). It should be noted that motor functions such as learning, planning and execution are cognition dependent. Indeed, studies have reported that activity in the prefrontal areas increased during motor tasks (Dirnberger et al., 2005; Sabatini et al., 2000). In patients with PD, regional cerebral blood flow (rCBF) decrease in the prefrontal cortex was associated with worse UPDRS-III scores (Kikuchi et al., 2001). Meanwhile, several studies (Canu et al., 2015; Wen et al., 2018) in PD patients who presented with tremor, freezing of gait, or walking difficulties demonstrated reduced FA in the gCC. Therefore, the disruption of the gCC may affect the executive function and aggravate motor impairments. Taken together, the aforementioned studies show that alterations in the gCC are very important for motor symptoms in PD patients.

The FD of the bilateral CST was higher in PD patients than in HCs. CST is an important projection fiber tract that controls motor movements. Interestingly, alterations in CST were rarely reported in previous studies in PD patients. Studies that performed either whole-brain comparisons (Ji et al., 2015; Perea et al., 2013), fiber tracking, or region-of-interest analysis (Lu et al., 2016; Nilsson et al., 2007) failed to find CST abnormality. It is possible that the alteration in the CST was not large enough and might have been masked by crossing fibers. Indeed, the CST runs vertically and crosses the SLF as well as several other fibers (Wiegell et al., 2000). Therefore, in voxels that contain both CST and other fibers that run horizontally, traditional tensor-based metrics might be less sensitive to CST-specific changes. By using FBA, we can directly assess alterations within specific fiber tracts, allowing us to reveal subtle alterations in a single fiber bundle. Moreover, we found that the mean FD values of the CST were positively correlated with the UPDRS-III scores. While the detailed mechanism underlying such an association still needs further clarification, it may be due to compensatory mechanisms. Because brain networks are dynamically organized, when certain parts of the motor circuitry are damaged, some other structures may reorganize or strengthen to compensate for the motor impairment. In stroke patients, increased CST integrity in the contralateral brain hemisphere may benefit stroke recovery (Fries et al., 1993). Increased cortical (Wu et al., 2015, 2015) and cerebellar activation (Rascol et al., 1997; Wu and Hallett, 2013) has been frequently reported in PD patients, which may compensate for the dysfunction of basal ganglia nucleus. Here our results suggested that the CST may be enhanced to make up for the loss of excitability in the cortical-striatal circuit. The increased FD of the CST was detected in both ES and MS PD patients, suggesting that the compensatory effect may start from ES and extend into the MS.

We also found that the log-FC of the SCP was significantly increased in PD patients compared to HCs. Additionally, the mean log-FC values of the SCP were positively correlated with the UPDRS-III scores. The SCP originates from deep cerebellar nuclei, including the fastigial nucleus, interpositus nucleus, and dentate nucleus (Steriade, 1995). The cerebellum is connected to other brain structures by white matter fibers and plays a crucial role in many functional networks, especially motor networks (Habas, 2010). Previous studies have shown that the

Table 2
Mean fixel values significant regions in ANOVA tests from all participants.

Index	ES		MS		HC		Post-hoc#		
	MEAN	SD	MEAN	SD	MEAN	SD	ES vs. MS#	ES vs. HC#	MS vs. HC#
FD of CST	0.723	0.057	0.759	0.068	0.683	0.066	0.025*	0.004*	< 0.001*
log-FC of SCP	−0.025	0.078	−0.016	0.084	−0.083	0.073	0.54	< 0.001*	< 0.001*

* $p < 0.05$.
\# Bonferroni correction.

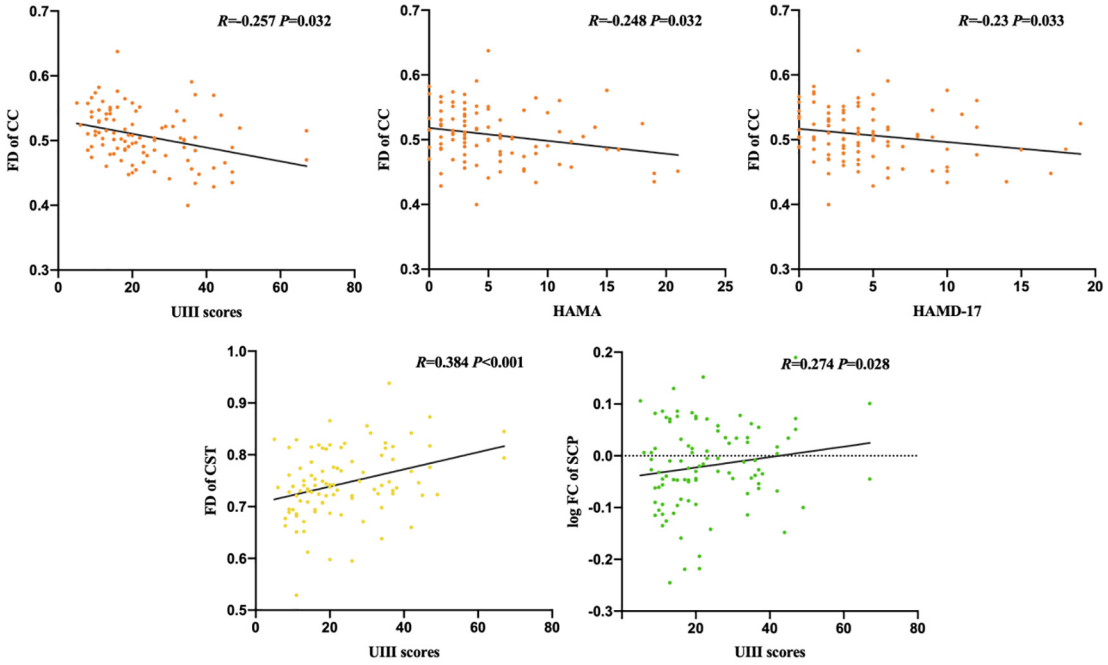

Fig. 4. Correlations between exacted values of mean FD and mean log FC of PD patients and clinical scales.

cerebellum and basal ganglia have distinct loops that are connected with largely overlapping areas, including the cerebral cortex (Percheron et al., 1996), striatum (Ichinohe et al., 2000), and subthalamic nucleus (Bostan et al., 2010). These connectivity patterns underlie the cerebellum's ability to compensate for the basal ganglia dysfunction. Middleton and Strick (2000) found that the cerebellum influenced motor function through the cerebello-thalamo-cortical circuit. Although alterations in SCP were rarely reported in previous studies involving PD patients, the cerebellum's compensatory effect was frequently reported. Yu et al. (2007) found, through task-based functional magnetic resonance imaging, that in PD patients with movement disorder, during exercise experiments, motor regions were inhibited while cerebellar regions were activated. Additionally, cerebellar hypermetabolism has been speculated to reflect compensatory activity to maintain motor functions (Wu and Hallett, 2013).

In a recent study, Rau et al. (2019) applied the FBA method to study longitudinal white matter fiber changes in PD patients. Their study involved 50 PD patients and two-year longitudinal observations. In comparison with 76 healthy controls, they did not find any significant alterations in PD patients. Longitudinal changes were found in the corpus callosum, tapetum, cingulum, and other regions. The degeneration of the corpus callosum reported in their study was generally consistent with our findings. It is worth noting that they also reported a temporary increase in FD/FC in several fiber tracts. The different cross-sectional results may partly be due to the different sample characteristics and acquisition schemes. Our study involved a larger sample size (98 patients), which may have enabled us to detect more changes. While the multi-shell acquisition scheme is better for resolving fiber orientations, the aforementioned study sacrificed some brain regions in order to scan the cerebrum, possibly due to the weak clinical scanner gradient and the inability of PD patients to tolerate long scan times. In the present study, we scanned the whole brain and found alterations in the cerebellar fiber tract.

Here we had not found alterations in the nigrostriatal and mesolimbic pathways, which are also common in most previous studies (Andica et al., 2019; Atkinson-Clement et al., 2017). It is possible that fibers connecting these structures are too thin to be found using routine dMRI acquisition and analysis method. Indeed, Tan et al. (2015) up-sampled the dMRI data to 1 mm^3, performed fiber tracking and revealed decreased FA in the Nigrostriatal-Nigropallidal pathway. Zhang et al. (2015) also up-sampled the dMRI data to 1 mm^3, and found decreased FA in the nigrostriatal pathway. While the up-sampling method may help detect changes in these pathways, its validity and reliability are yet to be confirmed. With the development of high-field imaging and multi-band acceleration method, studies using ultra-high resolution (~1mm) dMRI acquisition protocols may be ideal for answering this question.

In line with expectations, our findings suggest that PD patients exhibit both microstructural and macrostructural alterations in multiple white matter tracts. Based on these findings, we propose that white matter degeneration may occur in a specific pattern across different stages of PD (Fig. 5). The degeneration of dopaminergic neurons starts at the very beginning of PD development. As the disease progresses to the early stage of PD, basal ganglia functions are gradually impaired, and the CST compensates for the motor insufficiency. With further disease exacerbation, the CC degenerates continuously, and motor functions shift from the basal ganglia circuit towards the relatively preserved cerebellar circuit, leading to increased FC in the SCP. Indeed, these degeneration/compensation mechanisms have been

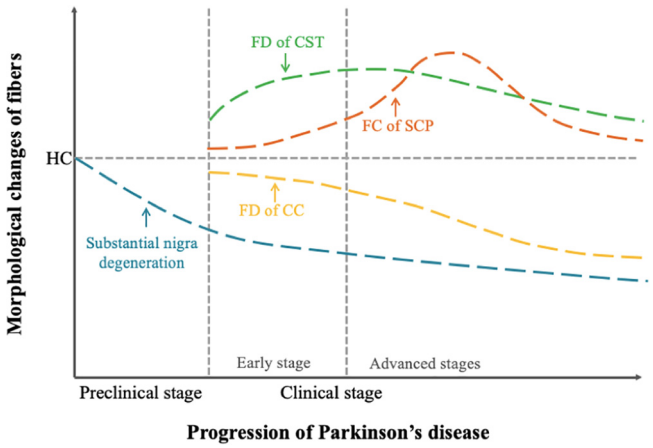

Fig. 5. Schematic diagram of fiber tract structural changes during the development Parkinson's disease.

demonstrated in previous studies (Doron and Gazzaniga, 2008; Middleton and Strick, 2000; Rau et al., 2019) that suggest the occurrence of a complicated brain re-organization process during PD progression. Further confirmation and elucidation of these changes may provide important insights into the unique development course of PD.

5. Limitations

There are a few limitations to our study. Patients in our MS PD group were older than those in the ES PD group. Although we regressed out the effect of age during general linear model analysis, the nonlinear effect may have acted as a confounding factor. Second, all our patients were right-handed. Therefore, the left CST was inherently more dominant than the right (Jang and Jang, 2016). This might be the reason why, among the three groups, a difference in the FD of the CST could only be found on the right side. Third, it should be noted that multi-shell and higher b-value data are ideal for accurately estimating fiber orientations. However, it may be difficult to acquire multi-shell dMRI data using clinical scanners, and some studies emphasized that data with a single b-value could also produce relatively robust results (Jeurissen et al., 2013; Tournier et al., 2007). Further multi-shell dMRI studies are needed to verify our findings.

6. Conclusion

In the present study, we implemented a novel dMRI analysis method and found that PD patients exhibited both axonal loss and growth within specific fiber pathways. Moreover, fiber alterations were different across disease stages and correlated with different clinical symptoms. The increase in FD in the CST and FC in the SCP suggests that the white matter may compensate for neuronal damage caused by PD pathology. Due to the exploratory nature of the present study, future studies are needed to validate our findings and clarify the related pathophysiological mechanisms.

CRediT authorship contribution statement

Yanxuan Li: Methodology, Software, Validation, Formal analysis, Investigation, Data curation, Visualization, Writing - original draft, Writing - review & editing. **Tao Guo:** Data curation. **Xiaojun Guan:** Data curation. **Ting Gao:** Data curation. **Wenshuang Sheng:** Data curation. **Cheng Zhou:** Data curation. **Jingjing Wu:** Data curation. **Min Xuan:** Data curation. **Quanquan Gu:** Data curation. **Minming Zhang:** Conceptualization, Funding acquisition. **Yunjun Yang:** Conceptualization, Funding acquisition. **Peiyu Huang:** Supervision, Conceptualization, Writing - original draft, Writing - review & editing, Funding acquisition, Project administration.

Acknowledgements

This study was supported by the 13th Five-year Plan for National Key Research and Development Program of China (Grant No. 2016YFC1306600), the National Natural Science Foundation of China (Grant Nos. 81771820 and 81701647), and the Natural Science Foundation of Zhejiang Province (Grant No. LSZ19H180001).

Appendix A. Supplementary data

Supplementary data to this article can be found online at https://doi.org/10.1016/j.nicl.2020.102355.

References

Albin, R.L., Young, A.B., Penney, J.B., 1989. The functional anatomy of basal ganglia disorders. Trends Neurosci. 12, 366–375. https://doi.org/10.1016/0166-2236(89)90074-x.

Alexander, G.E., Crutcher, M.D., 1990. Functional architecture of basal ganglia circuits: neural substrates of parallel processing. Trends Neurosci. 13, 266–271. https://doi.org/10.1016/0166-2236(90)90107-l.

Andica, C., Kamagata, K., Hatano, T., Saito, Y., Ogaki, K., Hattori, N., Aoki, S., 2019. MR biomarkers of degenerative brain disorders derived from diffusion imaging. J. Magn. Reson. Imaging.

Atkinson-Clement, C., Pinto, S., Eusebio, A., Coulon, O., 2017. Diffusion tensor imaging in Parkinson's disease: Review and meta-analysis. Neuroimage Clin. 16, 98–110. https://doi.org/10.1016/j.nicl.2017.07.011.

Beaulieu, C., 2014. The biological basis of diffusion anisotropy. Diffusion MRI. Elsevier 155–183.

Beaulieu, C., 2002. The basis of anisotropic water diffusion in the nervous system - a technical review. NMR Biomed. 15, 435–455. https://doi.org/10.1002/nbm.782.

Bertrand, J.-A., Bedetti, C., Postuma, R.B., Monchi, O., Genier Marchand, D., Jubault, T., Gagnon, J.-F., 2012. Color discrimination deficits in Parkinson's disease are related to cognitive impairment and white-matter alterations. Mov. Disord. 27, 1781–1788. https://doi.org/10.1002/mds.25272.

Bostan, A.C., Dum, R.P., Strick, P.L., 2010. The basal ganglia communicate with the cerebellum. Proc. Natl. Acad. Sci. U S A 107, 8452–8456. https://doi.org/10.1073/pnas.1000496107.

Braak, H., Bohl, J.R., Muller, C.M., Rub, U., de Vos, R.A.I., Del Tredici, K., 2006. Stanley Fahn Lecture 2005: The staging procedure for the inclusion body pathology associated with sporadic Parkinson's disease reconsidered. Mov. Disord. 21, 2042–2051. https://doi.org/10.1002/mds.21065.

Buhusi, C.V., Meck, W.H., 2005. What makes us tick? Functional and neural mechanisms of interval timing. Nat. Rev. Neurosci. 6, 755–765. https://doi.org/10.1038/nrn1764.

Canu, E., Agosta, F., Sarasso, E., Volontè, M.A., Basaia, S., Stojkovic, T., Stefanova, E., Comi, G., Falini, A., Kostic, V.S., Gatti, R., Filippi, M., 2015. Brain structural and functional connectivity in Parkinson's disease with freezing of gait. Hum. Brain Mapp. 36, 5064–5078. https://doi.org/10.1002/hbm.22994.

Chan, L.-L., Ng, K.-M., Rumpel, H., Fook-Chong, S., Li, H.-H., Tan, E.-K., 2014. Transcallosal diffusion tensor abnormalities in predominant gait disorder parkinsonism. Parkinsonism Relat. Disord. 20, 53–59. https://doi.org/10.1016/j.parkreldis.2013.09.017.

Dirnberger, G., Frith, C.D., Jahanshahi, M., 2005. Executive dysfunction in Parkinson's disease is associated with altered pallidal-frontal processing. Neuroimage 25, 588–599. https://doi.org/10.1016/j.neuroimage.2004.11.023.

Doron, K.W., Gazzaniga, M.S., 2008. Neuroimaging techniques offer new perspectives on callosal transfer and interhemispheric communication. Cortex 44, 1023–1029. https://doi.org/10.1016/j.cortex.2008.03.007.

Douaud, G., Jbabdi, S., Behrens, T.E.J., Menke, R.A., Gass, A., Monsch, A.U., Rao, A., Whitcher, B., Kindlmann, G., Matthews, P.M., Smith, S., 2011. DTI measures in crossing-fibre areas: increased diffusion anisotropy reveals early white matter alteration in MCI and mild Alzheimer's disease. Neuroimage 55, 880–890. https://doi.org/10.1016/j.neuroimage.2010.12.008.

Fries, W., Danek, A., Scheidtmann, K., Hamburger, C., 1993. Motor recovery following capsular stroke. Role of descending pathways from multiple motor areas. Brain 116 (Pt 2), 369–382. https://doi.org/10.1093/brain/116.2.369.

Funahashi, S., Andreau, J.M., 2013. Prefrontal cortex and neural mechanisms of executive function. J. Physiol. Paris 107, 471–482.

Gajamange, S., Raffelt, D., Dhollander, T., Lui, E., van der Walt, A., Kilpatrick, T., Fielding, J., Connelly, A., Kolbe, S., 2018. Fibre-specific white matter changes in multiple sclerosis patients with optic neuritis. Neuroimage Clin. 17, 60–68. https://doi.org/10.1016/j.nicl.2017.09.027.

Gattellaro, G., Minati, L., Grisoli, M., Mariani, C., Carella, F., Osio, M., Ciceri, E., Albanese, A., Bruzzone, M.G., 2009. White matter involvement in idiopathic Parkinson disease: a diffusion tensor imaging study. AJNR Am. J. Neuroradiol. 30, 1222–1226. https://doi.org/10.3174/ajnr.A1556.

Habas, C., 2010. Functional imaging of the deep cerebellar nuclei: a review. Cerebellum 9, 22–28. https://doi.org/10.1007/s12311-009-0119-3.

Hanaie, R., Mohri, I., Kagitani-Shimono, K., Tachibana, M., Azuma, J., Matsuzaki, J., Watanabe, Y., Fujita, N., Taniike, M., 2013. Altered microstructural connectivity of the superior cerebellar peduncle is related to motor dysfunction in children with autistic spectrum disorders. Cerebellum 12, 645–656. https://doi.org/10.1007/s12311-013-0475-x.

Hattori, T., Orimo, S., Aoki, S., Ito, K., Abe, O., Amano, A., Sato, R., Sakai, K., Mizusawa, H., 2012. Cognitive status correlates with white matter alteration in Parkinson's disease. Hum. Brain Mapp. 33, 727–739. https://doi.org/10.1002/hbm.21245.

Huang, P., Xu, X., Gu, Q., Xuan, M., Yu, X., Luo, W., Zhang, M., 2014. Disrupted white matter integrity in depressed versus non-depressed Parkinson's disease patients: a tract-based spatial statistics study. J. Neurol. Sci. 346, 145–148. https://doi.org/10.1016/j.jns.2014.08.011.

Hughes, A.J., Daniel, S.E., Kilford, L., Lees, A.J., 1992. Accuracy of clinical diagnosis of idiopathic Parkinson's disease: a clinico-pathological study of 100 cases. J. Neurol. Neurosurg. Psychiatry. 55, 181–184. https://doi.org/10.1136/jnnp.55.3.181.

Ibarretxe-Bilbao, N., Junque, C., Marti, M.-J., Valldeoriola, F., Vendrell, P., Bargallo, N., Zarei, M., Tolosa, E., 2010. Olfactory impairment in Parkinson's disease and white matter abnormalities in central olfactory areas: A voxel-based diffusion tensor imaging study. Mov. Disord. 25, 1888–1894. https://doi.org/10.1002/mds.23208.

Ichinohe, N., Mori, F., Shoumura, K., 2000. A di-synaptic projection from the lateral cerebellar nucleus to the laterodorsal part of the striatum via the central lateral nucleus of the thalamus in the rat. Brain. Res. 880, 191–197. https://doi.org/10.1016/s0006-8993(00)02744-x.

Innocenti, G.M., Manger, P.R., Masiello, I., Colin, I., Tettoni, L., 2002. Architecture and callosal connections of visual areas 17, 18, 19 and 21 in the ferret (Mustela putorius).

Cereb. Cortex 12, 411–422. https://doi.org/10.1093/cercor/12.4.411.
Jang, S.H., Jang, W.H., 2016. Change of the Corticospinal Tract in the Unaffected Hemisphere by Change of the Dominant Hand Following Stroke: A Cohort Study. Medicine (Baltimore) 95, e2620. https://doi.org/10.1097/MD.0000000000002620.
Jeurissen, B., Leemans, A., Tournier, J.-D., Jones, D.K., Sijbers, J., 2013. Investigating the prevalence of complex fiber configurations in white matter tissue with diffusion magnetic resonance imaging. Hum. Brain Mapp. 34, 2747–2766. https://doi.org/10.1002/hbm.22099.
Ji, L., Wang, Y., Zhu, D., Liu, W., Shi, J., 2015. White matter differences between multiple system atrophy (parkinsonian type) and Parkinson's disease: a diffusion tensor image study. Neuroscience 305, 109–116.
Johansen-Berg, H., Behrens, T.E., 2013. Diffusion MRI: from quantitative measurement to in vivo neuroanatomy. Academic Press.
Karagulle Kendi, A.T., Lehericy, S., Luciana, M., Ugurbil, K., Tuite, P., 2008. Altered diffusion in the frontal lobe in Parkinson disease. AJNR Am. J. Neuroradiol. 29, 501–505. https://doi.org/10.3174/ajnr.A0850.
Kikuchi, A., Takeda, A., Kimpara, T., Nakagawa, M., Kawashima, R., Sugiura, M., Kinomura, S., Fukuda, H., Chida, K., Okita, N., Takase, S., Itoyama, Y., 2001. Hypoperfusion in the supplementary motor area, dorsolateral prefrontal cortex and insular cortex in Parkinson's disease. J. Neurol. Sci. 193, 29–36. https://doi.org/10.1016/s0022-510x(01)00641-4.
Li, W., Liu, J., Skidmore, F., Liu, Y., Tian, J., Li, K., 2010. White matter microstructure changes in the thalamus in Parkinson disease with depression: A diffusion tensor MR imaging study. AJNR Am. J. Neuroradiol. 31, 1861–1866. https://doi.org/10.3174/ajnr.A2195.
Li, Y., Huang, P., Guo, T., Guan, X., Gao, T., Sheng, W., Zhou, C., Wu, J., Song, Z., Xuan, M., Gu, Q., Xu, X., Yang, Y., Zhang, M., 2019. Brain structural correlates of depressive symptoms in Parkinson's disease patients at different disease stage. Psychiatry Res. Neuroimag. 296, 111029. https://doi.org/10.1016/j.pscychresns.2019.111029.
Lu, M.-K., Chen, C.-M., Duann, J.-R., Ziemann, U., Chen, J.-C., Chiou, S.-M., Tsai, C.-H., 2016. Investigation of motor cortical plasticity and corticospinal tract diffusion tensor imaging in patients with Parkinsons disease and essential tremor. PLoS ONE 11.
Lyon, M., Welton, T., Varda, A., Maller, J.J., Broadhouse, K., Korgaonkar, M.S., Koslow, S.H., Williams, L.M., Gordon, E., Rush, A.J., Grieve, S.M., 2019. Gender-specific structural abnormalities in major depressive disorder revealed by fixel-based analysis. Neuroimage Clin. 21, 101668. https://doi.org/10.1016/j.nicl.2019.101668.
Melzer, T.R., Watts, R., MacAskill, M.R., Pitcher, T.L., Livingston, L., Keenan, R.J., Dalrymple-Alford, J.C., Anderson, T.J., 2013. White matter microstructure deteriorates across cognitive stages in Parkinson disease. Neurology 80, 1841–1849. https://doi.org/10.1212/WNL.0b013e3182929f62.
Middleton, F.A., Strick, P.L., 2000. Basal ganglia and cerebellar loops: motor and cognitive circuits. Brain Res. Brain Res. Rev. 31, 236–250. https://doi.org/10.1016/s0165-0173(99)00040-5.
Mito, R., Raffelt, D., Dhollander, T., Vaughan, D.N., Tournier, J.-D., Salvado, O., Brodtmann, A., Rowe, C.C., Villemagne, V.L., Connelly, A., 2018. Fibre-specific white matter reductions in Alzheimer's disease and mild cognitive impairment. England. https://doi.org/10.1093/brain/awx355.
Mori, S., Wakana, S., Van Zijl, P.C., Nagae-Poetscher, L.M., 2005. MRI atlas of human white matter. Elsevier.
Nilsson, C., Bloch, K.M., Brockstedt, S., Lätt, J., Widner, H., Larsson, E.-M., 2007. Tracking the neurodegeneration of parkinsonian disorders–a pilot study. Neuroradiology 49, 111–119.
Oishi, K., Zilles, K., Amunts, K., Faria, A., Jiang, H., Li, X., Akhter, K., Hua, K., Woods, R., Toga, A.W., 2008. Human brain white matter atlas: identification and assignment of common anatomical structures in superficial white matter. Neuroimage 43, 447–457.
Owen, A.M., 1997. Cognitive planning in humans: neuropsychological, neuroanatomical and neuropharmacological perspectives. Prog. Neurobiol. 53, 431–450. https://doi.org/10.1016/s0301-0082(97)00042-7.
Percheron, G., Francois, C., Talbi, B., Yelnik, J., Fenelon, G., 1996. The primate motor thalamus. Brain Res. Brain Res. Rev. 22, 93–181.
Perea, R.D., Rada, R.C., Wilson, J., Vidoni, E.D., Morris, J.K., Lyons, K.E., Pahwa, R., Burns, J.M., Honea, R.A., 2013. A comparative white matter study with Parkinson's disease, Parkinson's disease with dementia and Alzheimer's disease. J. Alzheimer's Dis. Parkinsonism 3, 123.
Rae, C.L., Correia, M.M., Altena, E., Hughes, L.E., Barker, R.A., Rowe, J.B., 2012. White matter pathology in Parkinson's disease: the effect of imaging protocol differences and relevance to executive function. Neuroimage 62, 1675–1684. https://doi.org/10.1016/j.neuroimage.2012.06.012.
Raffelt, D., Tournier, J.-D., Fripp, J., Crozier, S., Connelly, A., Salvado, O., 2011. Symmetric diffeomorphic registration of fibre orientation distributions. Neuroimage 56, 1171–1180. https://doi.org/10.1016/j.neuroimage.2011.02.014.
Raffelt, D., Tournier, J.-D., Rose, S., Ridgway, G.R., Henderson, R., Crozier, S., Salvado, O., Connelly, A., 2012. Apparent Fibre Density: a novel measure for the analysis of diffusion-weighted magnetic resonance images. Neuroimage 59, 3976–3994. https://doi.org/10.1016/j.neuroimage.2011.10.045.
Raffelt, D.A., Smith, R.E., Ridgway, G.R., Tournier, J.-D., Vaughan, D.N., Rose, S., Henderson, R., Connelly, A., 2015. Connectivity-based fixel enhancement: Whole-brain statistical analysis of diffusion MRI measures in the presence of crossing fibres. Neuroimage 117, 40–55. https://doi.org/10.1016/j.neuroimage.2015.05.039.
Raffelt, D.A., Tournier, J.-D., Smith, R.E., Vaughan, D.N., Jackson, G., Ridgway, G.R., Connelly, A., 2017. Investigating white matter fibre density and morphology using fixel-based analysis. Neuroimage 144, 58–73. https://doi.org/10.1016/j.neuroimage.2016.09.029.
Rascol, O., Sabatini, U., Fabre, N., Brefel, C., Loubinoux, I., Celsis, P., Senard, J.M., Montastruc, J.L., Chollet, F., 1997. The ipsilateral cerebellar hemisphere is overactive during hand movements in akinetic parkinsonian patients. Brain 120 (Pt 1), 103–110. https://doi.org/10.1093/brain/120.1.103.
Rau, Y.-A., Wang, S.-M., Tournier, J.-D., Lin, S.-H., Lu, C.-S., Weng, Y.-H., Chen, Y.-L., Ng, S.-H., Yu, S.-W., Wu, Y.-M., 2019. A longitudinal fixel-based analysis of white matter alterations in patients with Parkinson's disease. NeuroImage: Clinical 24, 102098.
Sabatini, U., Boulanouar, K., Fabre, N., Martin, F., Carel, C., Colonnese, C., Bozzao, L., Berry, I., Montastruc, J.L., Chollet, F., Rascol, O., 2000. Cortical motor reorganization in akinetic patients with Parkinson's disease: a functional MRI study. Brain 123 (Pt 2), 394–403. https://doi.org/10.1093/brain/123.2.394.
Smith, R.E., Tournier, J.-D., Calamante, F., Connelly, A., 2013. SIFT: Spherical-deconvolution informed filtering of tractograms. Neuroimage 67, 298–312. https://doi.org/10.1016/j.neuroimage.2012.11.049.
Steriade, M., 1995. Two channels in the cerebellothalamocortical system. J Comp Neurol 354, 57–70. https://doi.org/10.1002/cne.903540106.
Tan, W.-Q., Yeoh, C.-S., Rumpel, H., Nadkarni, N., Lye, W.-K., Tan, E.-K., Chan, L.-L., 2015. Deterministic Tractography of the Nigrostriatal-Nigropallidal Pathway in Parkinson's Disease. Sci. Rep. 5, 17283. https://doi.org/10.1038/srep17283.
Tanji, J., Shima, K., Mushiake, H., 2007. Concept-based behavioral planning and the lateral prefrontal cortex. Trends Cogn. Sci. 11, 528–534. https://doi.org/10.1016/j.tics.2007.09.007.
Tournier, J.-D., Calamante, F., Connelly, A., 2007. Robust determination of the fibre orientation distribution in diffusion MRI: non-negativity constrained super-resolved spherical deconvolution. Neuroimage 35, 1459–1472. https://doi.org/10.1016/j.neuroimage.2007.02.016.
Tustison, N.J., Avants, B.B., Cook, P.A., Zheng, Y., Egan, A., Yushkevich, P.A., Gee, J.C., 2010. N4ITK: improved N3 bias correction. IEEE Trans. Med Imaging 29, 1310–1320. https://doi.org/10.1109/TMI.2010.2046908.
Veraart, J., Fieremans, E., Novikov, D.S., 2016. Diffusion MRI noise mapping using random matrix theory. Magn. Reson. Med. 76, 1582–1593. https://doi.org/10.1002/mrm.26059.
Vercruysse, S., Leunissen, I., Vervoort, G., Vandenberghe, W., Swinnen, S., Nieuwboer, A., 2015. Microstructural changes in white matter associated with freezing of gait in Parkinson's disease. Mov. Disord. 30, 567–576. https://doi.org/10.1002/mds.26130.
Wen, M.-C., Heng, H.S.E., Lu, Z., Xu, Z., Chan, L.L., Tan, E.K., Tan, L.C.S., 2018. Differential White Matter Regional Alterations in Motor Subtypes of Early Drug-Naive Parkinson's Disease Patients. Neurorehabil. Neural Repair 32, 129–141. https://doi.org/10.1177/1545968317753075.
Wiegell, M.R., Larsson, H.B., Wedeen, V.J., 2000. Fiber crossing in human brain depicted with diffusion tensor MR imaging. Radiol. 217, 897–903. https://doi.org/10.1148/radiology.217.3.r00nv43897.
Wu, T., Hallett, M., 2013. The cerebellum in Parkinson's disease. Brain 136, 696–709. https://doi.org/10.1093/brain/aws360.
Wu, T., Hou, Y., Hallett, M., Zhang, J., Chan, P., 2015. Lateralization of brain activity pattern during unilateral movement in Parkinson's disease. Hum. Brain Mapp. 36, 1878–1891.
Yamauchi, H., Fukuyama, H., Nagahama, Y., Katsumi, Y., Dong, Y., Konishi, J., Kimura, J., 1997. Atrophy of the corpus callosum, cognitive impairment, and cortical hypometabolism in progressive supranuclear palsy. Ann. Neurol. 41, 606–614. https://doi.org/10.1002/ana.410410509.
Yin, H.H., Knowlton, B.J., 2006. The role of the basal ganglia in habit formation. Nat. Rev. Neurosci. 7, 464–476. https://doi.org/10.1038/nrn1919.
Yu, H., Sternad, D., Corcos, D.M., Vaillancourt, D.E., 2007. Role of hyperactive cerebellum and motor cortex in Parkinson's disease. Neuroimage 35, 222–233.
Zhang, G., Zhang, Y., Zhang, C., Wang, Y., Ma, G., Nie, K., Xie, H., Liu, J., Wang, L., 2015. Diffusion Kurtosis Imaging of Substantia Nigra Is a Sensitive Method for Early Diagnosis and Disease Evaluation in Parkinson's Disease. Parkinsons Dis. 2015, 207624. https://doi.org/10.1155/2015/207624.
Zhao, J., Liu, J., Jiang, X., Zhou, G., Chen, G., Ding, X.P., Fu, G., Lee, K., 2016. Linking Resting-State Networks in the Prefrontal Cortex to Executive Function: A Functional Near Infrared Spectroscopy Study. Front Neurosci. 10, 452. https://doi.org/10.3389/fnins.2016.00452.